Composites: Part A 39 (2008) 1065–1070

Contents lists available at ScienceDirect

Composites: Part A

journal homepage: www.elsevier.com/locate/compositesa

Short communication

Joining prepreg composite interfaces with aligned carbon nanotubes

Enrique J. Garcia, Brian L. Wardle *, A. John Hart

Massachusetts Institute of Technology, 77 Mass Avenue, MIT 33-314, Cambridge, MA-02139, USA

ARTICLE INFO

Article history:
Received 7 January 2008
Received in revised form 12 March 2008
Accepted 21 March 2008

Keywords:
A. Nano-structures
A. Hybrid
A. 3-Dimensional reinforcement
A. Fracture toughness

ABSTRACT

An interlaminar reinforcement using aligned carbon nanotubes (CNTs) is demonstrated for prepreg unidirectional carbon tape composites. Aligned CNTs are grown at high temperature and then transfer-printed to prepreg at room temperature, maintaining CNT alignment in the through-thickness direction. In initial testing, the CNT-modified interface is observed to increase fracture toughness 1.5–2.5X in Mode I, and 3X in Mode II. Both compliant interlayer and bridging are considered as mechanisms of toughening, with evidence of CNT bridging observed in fracture micrographs. Fabrication methods are compatible with existing manufacturing processes and have the potential to enhance the structural and multifunctional properties of advanced composite laminates.

1. Introduction

New structural concepts harnessing the attractive properties of carbon nanotubes (CNTs) have been pursued with great vigor in recent years [1–7]. In this work, a processing route for a hybrid advanced composite architecture is introduced utilizing standard prepreg-based manufacturing combined with aligned CNTs. The hybrid system (see Fig. 1) has three parts: advanced (carbon) fibers, an aerospace-grade polymer resin, and aligned CNTs oriented perpendicular to the ply surface (i.e., in the *z*-direction) to reinforce the laminate's interlaminar properties. The hybrid composite would not be considered a nanocomposite (comprised solely of CNTs and a matrix) [1,8,9], but rather a nano-engineered hybrid composite. The processes developed (see Fig. 2) utilize a rolling transfer scheme to transfer the aligned CNTs to the prepreg, potentially allowing integration into existing processing routes. Mode I and II fracture testing, and fracture-surface inspection are performed to investigate operative toughening mechanisms.

The development of composites utilizing CNTs has been hindered by difficulties in dispersing CNTs in polymers at high weight fractions while achieving uniform and strong interactions with the polymer matrix [1,3]. Studies of hybrid composites using unoriented CNTs dispersed in polymers report only marginal mechanical property improvements [10,11] at low CNT loadings. Thus, to realize mechanical improvements that take advantage of CNT properties, the CNTs should be aligned and organized with long-range order [12]. One approach to establishing such order is by spinning yarns or ropes of discontinuous CNTs [13,14] as a new type of advanced carbon 'fiber'. Another approach is to modify existing advanced composite systems to create hybrids. Dispersion and alignment challenges for nanocomposites are even more pronounced when the CNTs must be processed into a matrix with a high volume fraction (around 60%) of advanced fibers. The interface between plies in advanced composites is far more accessible from a processing standpoint than the laminate interior, and several studies have realized marginal to significant nano-modified interfacial properties using carbon nanofibers (CNFs) and CNTs at laminate interfaces [11,15–18]. Our approach is the first to integrate aligned CNTs with existing carbon fiber prepreg materials and processing. This is accomplished by growing a vertically-aligned CNT (VACNT) forest at high temperature, and then 'transfer-printing' the CNTs to prepreg at room temperature, taking advantage of the tack of the prepreg to separate the CNTs from the growth substrate (see Fig. 2). Our prior studies using off-the-shelf commercial complex thermosets indicate that aligned CNT forests readily draw up such polymers through capillary action [21], and bond to the resin [9].

2. Experimental

Fabrication of the VACNT-reinforced laminates is first presented, followed by the procedures used to test the laminates in Mode I and II. Two aerospace-grade unidirectional prepregs (Cytec IM7/977-3 and Hexcel AS4/8552) are used in Mode I, and AS4/8552 is utilized for Mode II. All SEM images were taken with a FEI/Philips XL30 FEG.

2.1. Laminate fabrication

CNTs are grown on a Si substrate using thermal chemical vapor deposition (CVD) of C_2H_4/H_2 at atmospheric pressure [23]. A

* Corresponding author. Tel.: +1 617 252 1539.
E-mail address: wardle@mit.edu (B.L. Wardle).

1359-835X/$ - see front matter © 2008 Elsevier Ltd. All rights reserved.
doi:10.1016/j.compositesa.2008.03.011

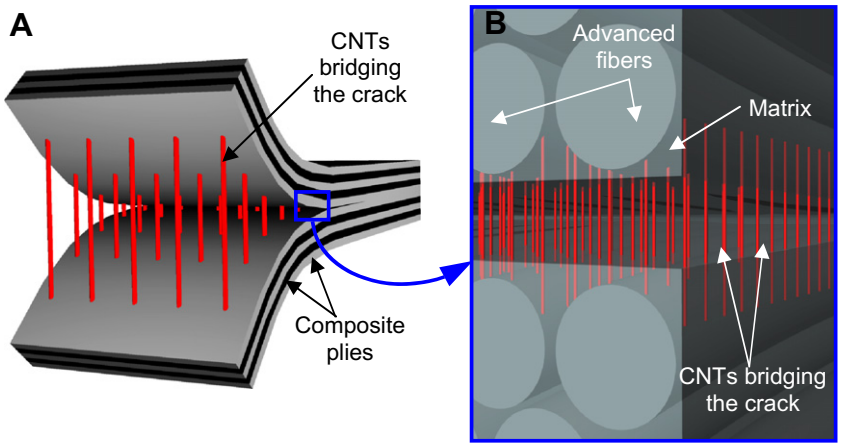

Fig. 1. Illustration of the ideal hybrid interlaminar architecture: (A) VACNTs placed in between two plies of a laminated composite; and (B) close-up of the crack, showing VACNTs bridging the crack between the two plies. Illustrations are not to scale.

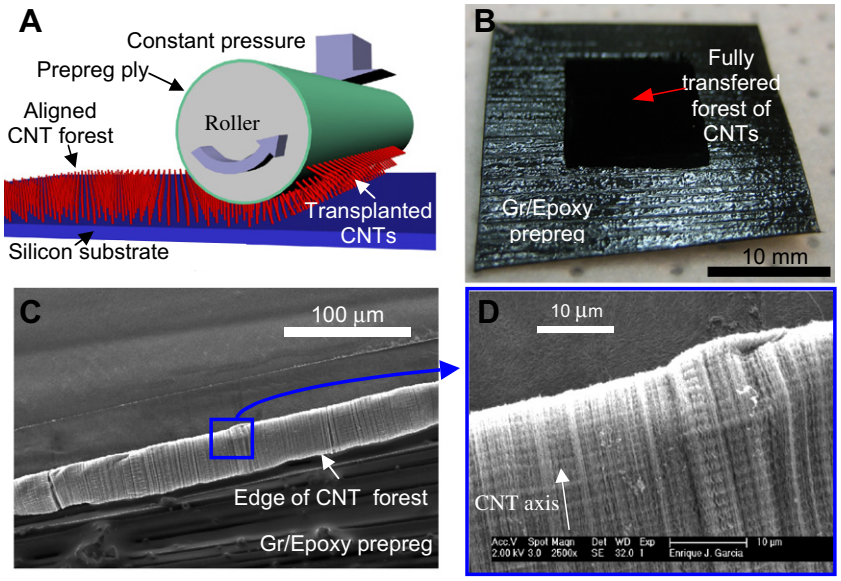

Fig. 2. Transfer-printing of VACNTs to prepreg: (A) Illustration of the 'transfer-printing' process; (B) CNT forest fully transplanted from its original silicon substrate to the surface of a Gr/Ep prepreg ply; (C and D) SEM images of the CNT forest, showing CNT alignment after transplantation.

continuous catalyst layer of 1.2/20 nm Fe/Al_2O_3 is deposited by electron beam evaporation to standard Si wafers. The wafers are cut into 30×20 mm pieces to fit in the quartz tube furnace (22 mm diameter). The CNTs grow through a base-growth mechanism and therefore are continuous top to bottom, having an average outer diameter of 8 nm [24] and are spaced an average of ~80 nm apart, giving a typical aligned-fiber volume fraction for the CNTs of ~1%. In previous studies, we have grown VACNTs as tall as 5 mm at average rates of 2 μm/s; however, it is believed that the ideal aligned CNT reinforcement would be comprised of short forests (<20 μm). As discussed in Section 3, the CNTs penetrate each ply by ~10 μm; therefore, an ~20 μm forest would introduce no additional thickness to the ply interlayer, which is commonly known to be detrimental to in-plane properties. For this initial study, longer CNTs (60–150 μm long) than desired were used due to limitations in growing short forests given the high CNT growth rate. The VACNTs are transplanted to a prepreg ply using exclusively mechanical means. The prepreg is attached to a cylinder that is rolled, while pressure is applied, across the Si substrate containing the CNT forest to transfer the CNTs (see Fig. 2A) to the tacky prepreg. Transfer rate, pressure, and geometry were varied until full transplantation of the CNT forest was achieved, as shown in Fig. 2B. The CNT forest maintains vertical alignment after transplantation and is neither broken nor buckled, as shown in the SEM images in Fig. 2C and D. The transplantation was equally effective and repeatable for the two prepregs. It should be noted that the CNTs are as-grown, i.e., unfunctionalized.

Before manufacturing laminates for fracture testing, a wetting test (epoxy from prepreg into the CNT forest) of mechanically transplanted CNTs is performed. A 20 mm square forest of 100 μm long CNTs was transplanted to a IM7/977-3 unidirectional prepreg strip (single ply). A second ply creates a 2-ply laminate with an aligned CNT interlayer. The laminate was assembled with appropriate cure materials and an aluminum caul plate and cured in an autoclave following the manufacturer recommendations (100 psig of total pressure, 15 psig vacuum, heat at 5 °F/min to 355 °F, hold for 6 h, cool at 5 °/min to 140 °F and vent pressure, let cool to room temperature). The laminate was diesawed using a DAD-2H/6T disco abrasive system (wafer diesaw). Both optical and scanning electron microscopy indicates that polymer from

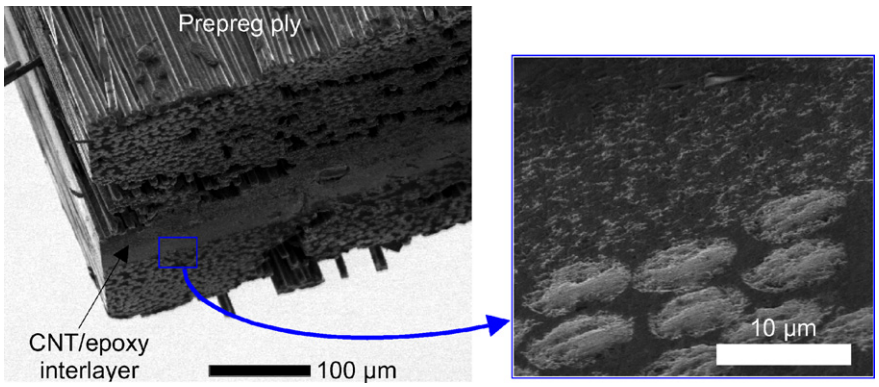

Fig. 3. SEM image of a 2-ply aligned CNT-interlayer hybrid composite fabricated to assess wetting of the CNT interlayer, showing a CNT/epoxy interlayer in between the two unidirectional carbon fiber prepreg plies.

the two prepreg plies is drawn into the aligned CNT forest to create an aligned CNT nanocomposite interlayer (see Fig. 3). The inset in Fig. 3 is of the interface between the lower ply (bottom of image, carbon fiber cross-sections clearly visible) and the CNT-epoxy interlayer. Two different color epoxy regions are clearly visible (upper containing CNTs, lower between the carbon fibers containing no CNTs) in the SEM due to the change in conductance caused by the CNTs. The height of the CNT interlayer is approximately that of the CNT forest before curing, so it is inferred that the CNTs maintain their alignment after the cure cycle. *In situ* visualization of CNT alignment using TEM has been unsuccessful due to sample preparation (focused ion beam – FIB, cryogenic microtome, and polishing) issues associated with the hardness and stiffness differences of the carbon fibers and CNT-epoxy.

The same overall procedure given above is used to fabricate laminates for fracture testing. First, 160 mm × 20 mm strips of unidirectional IM7/977-3 and AS4/8552 prepreg tape were cut and stacked to create two 12-layer laminates. A 90 × 20 mm CNT forest (three 30 × 20 mm forests) 60, 120, or 150 μm high was transplanted from the silicon substrate to one of the two 12-layer laminates, leaving a 50 × 20 mm section where a 13 μm sheet of Teflon was placed as a crack initiator. The two laminate stacks were assembled together, forming a 140 mm long by 20 mm wide 24-layer composite laminate plus CNT interlayer with a ~50 mm long precrack at the mid-plane from the Teflon insert. The curing cycle for the IM7/977-3 has been described above, and for AS4/8552, vacuum (15 psig) was applied, and the specimens were cured following the manufacturer recommendations (100 psig of total pressure, heat at 5 °F/min to 355 °F, hold for 2.5 h, cool at 5 °F/min to 140 °F and vent pressure, let cool to room temperature). After curing, the specimens were trimmed and paint applied on the edges to mark regular distances from the precrack.

2.2. Fracture testing

Experiments were performed to compare fracture behavior of laminates with and without aligned CNT interlayers. Mode I fracture tests [19] were applied to double cantilever (DCB) specimens at a constant crosshead speed. Four point bending tests on end notched flexure (4ENF) specimens were used to determine Mode II fracture toughness [20]. In the 4ENF testing procedure, the specimen is loaded and unloaded sequentially to propagate the crack. In this manner, rather than a pure propagating crack, the crack is opened and closed repeatedly to advance the crack. The 4ENF test yields an R-curve with stable crack propagation relative to the unstable growth associated with a 3ENF test [20]. In all cases the laminates were simple 0° laminates with all plies having fibers oriented in the direction of crack advance per the testing guidance. For the DCB test, an Instron 8848 MicroTester with a calibrated 2 kN load cell was used to perform the fracture tests at a constant crosshead speed of 0.5 mm/min. The microtester has range 5–2 kN, with resolution of 1 mN for load and 1 μm for displacement. Load, displacement, and crack propagation are measured until the crack is grown more than 20 mm per the standard and toughness is calculated using the compliance calibration method following the standard [19]. For the Mode II tests, a four point bending setup is used at a constant crosshead speed of 0.3 mm/min. The load is applied until the crack advances 3 mm, and then the specimen is unloaded to the initial position at a constant crosshead speed of 0.5 mm/min. This process is repeated several times to obtain Mode II R-curves, and toughness is calculated following the ENF guidelines in [20].

3. Results and discussion

The fabrication of aligned CNTs oriented perpendicular to the interface is a key aspect of the observed fracture behavior to be discussed subsequently. After the VACNTs are transfer-printed to the prepreg, laminate assembly and curing proceeds per the manufacturer's recommended processing with no modifications. CNT alignment on the prepreg has been confirmed using SEM and discussed previously (see Fig. 2). It was also shown that the aligned CNTs are wet by epoxy from just two plies of prepreg (see Fig. 3) to form an interlayer. Similar to the 2-ply system, 24-ply laminates manufactured for fracture testing also exhibit an interlayer of CNTs and

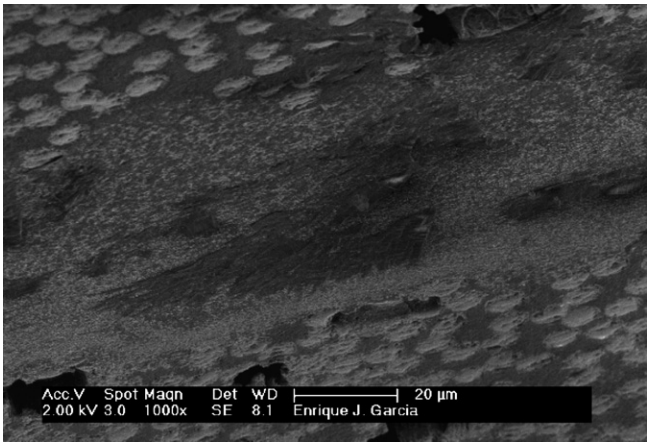

Fig. 4. SEM cross-sectional view of IM7/977-3 laminate midplane reinforced with a 60 μm aligned CNT forest.

Table 1
Summary of preliminary mode I and mode II fracture testing

Test type	Material system	# Specimens (baseline/hybrid)	Average CNT height (μm)	Baseline initiation toughness (kJ/m^2)	Baseline 0° toughened (kJ/m^2)	Hybrid toughness (kJ/m^2)	Apparent increase in toughness
Mode I	IM7/977-3	3/1	60	0.21	0.37	0.53	2.5X
	AS4/8552	3/2	150	0.21	0.25	0.34	1.5X
Mode II	AS4/8552	2/2	120	0.35	N/A	1.1	3X

polymer as shown in Fig. 4. Here, the CNT forest introduced at the laminate midplane is ~60 μm in average height, and the interlayer formed after autoclave processing is observed to be approximately this thickness as well. Equal thickness CNT forests and interlayers are observed for other specimens, perhaps indicating that overall CNT alignment is maintained. However, as discussed previously, direct visualization of CNT alignment at the interlayer has been unsuccessful. In the following discussion of fracture-surface morphology, aligned CNTs are observed in post-mortem Mode I fracture inspections. The VACNTs are wet by the epoxy contained in the prepreg and penetrate the ply structure 10–20 μm (see Figs. 3 and 4). Given the CNT size and spacing, ~25 CNTs can fit into every 2 μm between carbon fibers. The VACNTs may act as interlaminar nano *z*-fibers/*z*-pins, termed here 'interlaminar nanostitches'.

Mode I and II fracture tests were carried out on a small number of specimens due to the initially difficult and time-consuming nature of the hybrid laminate fabrication. For both material systems and in Mode I and II, hybrid laminates with CNTs displayed increased fracture toughness over the baseline laminates (see Table 1). Example R-curves from Mode I and II tests are given in Fig. 5. Initiation toughness in Mode I is found to be comparable for the unreinforced and CNT-reinforced specimens as expected, while no distinction is noted in Mode II for initiation vs. propagation. This latter point is consistent with other reported data on prepreg tape in Mode II using the 4ENF test, where a Mode I pre-crack is intro-

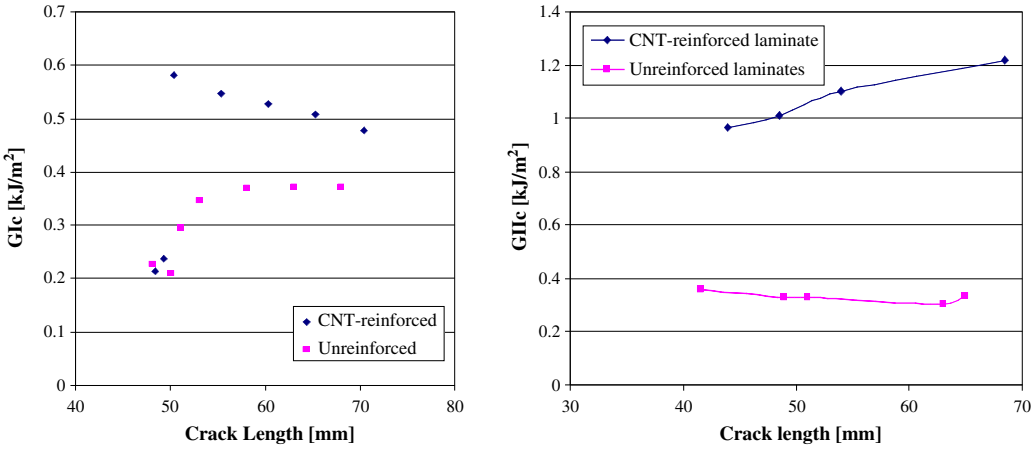

Fig. 5. Example R-curves for baseline and CNT-reinforced prepreg laminates: (A) Mode I IM7/977-3; and (B) Mode II AS4/8552.

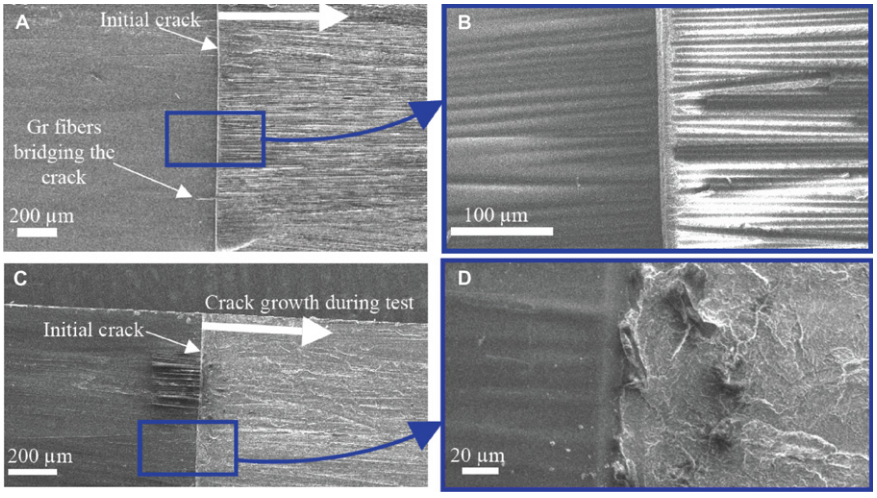

Fig. 6. SEM images of AS4/8552 Mode I fracture surfaces: (A) crack surface of unreinforced specimen; and (B) closer view of the initial crack; (C) crack surface of a CNT-reinforced specimen; and (D) Closer view of the reinforced crack surface.

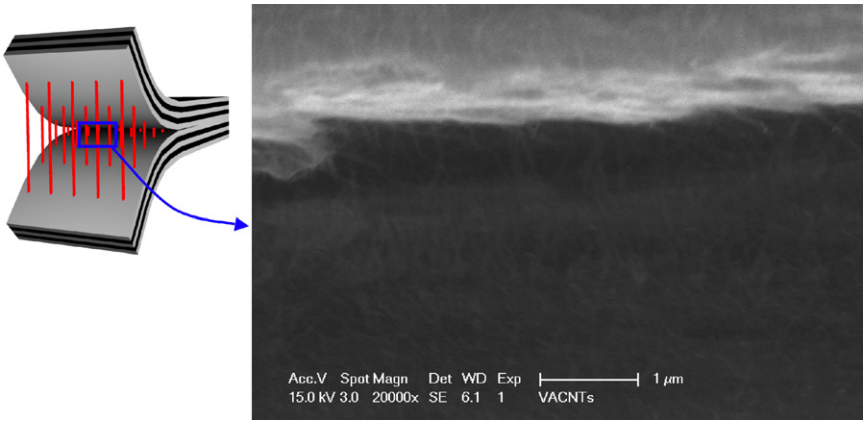

Fig. 7. SEM image of crack cross-section after Mode I fracture test of a hybrid AS4/8552 laminate. Visible on both the top and bottom surface are aligned CNT bundles. The crack has propagated between the CNT-epoxy interlayer (top of image) and the Gr/Ep ply (bottom of image).

duced prior to Mode II loading. The slightly decreasing R-curve in Fig. 5 for the Mode I hybrid laminate is attributed to the side-by-side nature (3 CNT forest patches placed side by side as discussed previously) of the CNT reinforcement. While in all cases toughness is noted to increase, the amount of increase needs further investigation with a larger number of samples and more consistent CNT interlayer fabrication (e.g., heights vary as shown in Table 1). Although incompatible with prepreg, large toughness enhancement has been observed with reinforcement of a SiC/epoxy by direct growth of large diameter (60 nm, vs. 8 nm here) partially-aligned CNTs on the surface of cloth [17].

Examination of the fracture surfaces from the Mode I tests provides insight into the possible toughening mechanisms at work. Two toughening mechanisms are considered: interlayer toughening via plastic deformation, and crack bridging. Both mechanisms can lead to significant toughening, as demonstrated by analysis and testing of stitched and *z*-fiber reinforced laminates [25] and numerous investigations of compliant interlayers/interleaves, e.g., [31]. Interleaving has the drawback of decreasing in-plane laminate properties, especially for thicker interlayers where more toughening is observed. Bridging is one of the most effective toughening mechanism known [22], and in stitching and *z*-fiber reinforcement [25], through-thickness properties generally increase significantly with the number of stitches (characterized by stitch spacing/density or volume fraction [26–28]), while in-plane properties are increasingly degraded as stitch density increases due to stitch insertion damage and interaction [29,30]. Thus, both toughening approaches, as is well known, have drawbacks particularly with regard to in-plane properties. Due to CNT forest synthesis constraints, particularly the large areas needed to create a fully-covered tensile specimen, in-plane properties of the CNT-reinforced laminates are not yet characterized.

Fracture surfaces of baseline and hybrid composites tested in Mode I are shown in Fig. 6. In Fig. 6A and B, the fracture surfaces indicate the expected toughening mechanism of 0° fiber bridging at the interface, a type of bridging caused by the co-linear 0° carbon fibers nesting between one another during laminate consolidation. Carbon fibers, and particularly their indentations in epoxy, are visible in Fig. 6B. This bridging is only present for 0°/0° interfaces and is a known artifact of the test standard. In Fig. 6C and D for the hybrid laminate, clear differences are observed relative to the interface without CNTs. The crack in the hybrid laminates is noted to propagate at one of the interlayer/ply interfaces (with no 0° fiber bridging, of course). A view looking into the crack opening for a hybrid Mode I specimen under SEM (see Fig. 7) reveals *z*-direction oriented CNTs on both crack faces, suggesting large-scale bridging of the crack by the (aligned) CNTs. Thus, both CNT bridging and interlayer toughening are possible reinforcing mechanisms, with direct evidence supporting CNT bridging.

4. Conclusions and recommendations

The interlaminar nanostitched architecture introduced here is realized by introducing VACNTs at the interface between plies of common prepreg material using a simple transfer-printing scheme. Preliminary Mode I and II tests indicate enhanced toughness, mechanistically explained by either interleaving or bridging toughening. CNTs observed on either surface of a Mode I crackface suggest bridging by pullout. While preliminary due to small sample size, the stable (toughened) critical energy release rate of the nanostitched architecture improves 3X in Mode II over the baseline laminate, which is greater than the typical improvement noted for standard stitching (<1X) [25,27] and *z*-fiber reinforcement (1X) [25,28] at comparable stitch densities of ~1% aligned reinforcement volume fraction (at higher stitch densities, Mode II toughness can increase much more significantly). Mode II toughness is a critical parameter for laminated composites as it affects delamination and impact damage resistance. Clearly, more refined specimen manufacturing and additional characterization are needed to appropriately quantify toughening and the mechanisms at work. Of great interest is fabricating shorter aligned CNT forests to reduce the interlayer thickness and thereby focus on bridging. Concomitant with producing shorter CNT forest reinforcement will be in-plane property measurement of laminate modulus and strength. Characterization and modeling of the enhanced properties afforded by this architecture could be extended and broadened to properties such as thermal [32] and electrical conductivity. Significant modeling [33] and experimentation still remains to determine optimal characteristics of the VACNTs including length and volume fraction, effects of chemical functionalization, and dependence on polymer chemistry and fiber surface characteristics. The interlaminar reinforcement presented here likely has application in several areas including bonded joints and repair of composites, as well as bonding of embedded or surface-mounted devices.

Acknowledgements

This work was supported by Airbus S.A.S., Boeing, Embraer, Lockheed Martin, Saab AB, Spirit AeroSystems, and Textron Inc. through MIT's Nano-Engineered Composite aerospace Structures (NECST) Consortium and by MIT's Karl Chang (1965) Innovation Fund. The authors gratefully thank John Kane, Namiko Yamamoto, and the entire Technology Laboratory for Advanced Materials and

Structures (TELAMS) at MIT for valuable discussions and technical support, Dr. Alexander H. Slocum for valuable input, and Dr. Roberto Guzman de Villoria for the CNT bridging SEM. Enrique Garcia acknowledges support from the La Caixa Foundation, and John Hart from the Fannie and John Hertz Foundation.

References

[1] Ajayan PM, Tour JM. Nanotube composites. Nature 2007;447:1066–8.
[2] Iijima S. Helical microtubules of graphitic carbon. Nature 1991;354:56–8.
[3] Schulte K, Windle AH. Editorial. Comp Sci Tech 2007;67:777.
[4] Lavine M. The right combination. Science 2006;314(5802):1099.
[5] Coleman JN, Khan U, Blau WJ, Gun'ko YK. Small but strong: a review of the mechanical properties of carbon nanotube–polymer composites. Carbon 2006;44:1624–52.
[6] Thostenson ET, Reng Z, Chou TW. Advances in the science and technology of carbon nanotubes and their composites: a review. Comp Sci Tech 2001;61:1899–912.
[7] Thostenson ET, Li C, Chou TW. Nanocomposites in context. Comp Sci Tech 2005;65:491–516.
[8] Vaia RA, Wagner HD. Framework for nanocomposites. Mater Today 2004;32:32–7.
[9] Garcia EJ, Hart AJ, Wardle BL, Slocum AH. Fabrication and nanocompression testing of aligned CNT/polymer nanocomposites. Adv Mater 2007;19:2151–6.
[10] Qiu J, Zhang C, Wang B, Liang R. Carbon nanotube integrated multifunctional composites. Nanotechnology 2007;18:275708–19.
[11] Beyakrova E, Thostenson ET, Yu A, Kim H, Gao J, Tang J, et al. Multiscale carbon nanotube-carbon fiber reinforcement for advanced epoxy composites. Langmuir 2007;23:3970–4.
[12] Windle AH. Two defining moments: a personal view from Prof. Alan H. Windle. Comp Sci Tech 2007;67:929–30.
[13] Li YL, Kinloch IA, Windle AH. Direct spinning of carbon nanotube fibers from chemical vapor deposition synthesis. Science 2004;304:276–8.
[14] Zhang M, Atkinson KR, Baughman R. Multifunctional carbon nanotube yarns by downsizing an ancient technology. Science 2004;306:1358–61.
[15] Adhikari K, Hubert P, Simard B, Johnston A. Effect of the localized application of SWNT modified epoxy on the interlaminar shear strength of carbon fiber laminates. In: 47th AIAA structures, dynamics, and materials conference proceedings, Newport, RI, May 1–4; 2006 [AIAA-2006-1855-604].
[16] Thakre PR, Lagoudas DC, Zhu J, Barrera EV. Processing and characterization of epoxy-SWCNT-woven fabric composites. In: 47th AIAA structures, dynamics, and materials conference proceedings, Newport, RI, May 1–4; 2006 [AIAA-2006-1857-212].
[17] Veedu VP, Cao A, Li X, Ma K, Soldano C, Kar S, et al. Multifunctional composites using reinforced laminae with carbon-nanotube forests. Nature Mat 2006;5:457–62.
[18] Zhu J, Imam A, Crane R, Lozano K, Khabasheku VN, Barrera EV. Processing a glass fiber-reinforced vinyl ester composite with nanotube enhancement of interlaminar shear strength. Comp Sci Tech 2007;67:1509–17.
[19] ASTM D 5528-01, Standard test method for mode I interlaminar fracture toughness of unidirectional fiber-reinforced polymer matrix composites. ASTM Int.
[20] Adams DF, Carlsson LA, Pipes RB. Experimental characterization of advanced composite materials. Boca Raton: CRC Press; 2003.
[21] Garcia EJ, Hart AJ, Wardle BL, Slocum AH. Fabrication of composite microstructures by capillarity-driven wetting of aligned carbon nanotubes with polymers. Nanotechnology 2007;18:165602.
[22] Anderson TL. Fracture mechanics: fundamentals and applications. 3rd ed. CRC Press; 1995.
[23] Hart AJ, Slocum AH. Flow-mediated nucleation and rapid growth of millimeter-scale aligned carbon nanotube structures from a thin-film catalyst. J Phys Chem B 2006;110:8250–7.
[24] Wang BN, Bennett RD, Verploegen E, Hart AJ, Cohen RE. Quantitative characterization of the morphology of multiwall carbon nanotube films by small-angle X-ray scattering. J Phys Chem C 2007;111(16):5859–65.
[25] Tong L, Mouritz AP, Bannister MK. In: 3D fiber-reinforced polymer composites. Oxford: Elsevier; 2002 [Fig. 8.10.].
[26] Dransfield KA, Jain LK, Mai YW. On the effects of stitching in CFRPs—I. Mode I delamination toughness. Comp Sci Tech 1998;58:815–27.
[27] Jain LK, Dransfield KA, Mai YW. On the effects of stitching in CFRPs—II. Mode II delamination toughness. Comp Sci Tech 1998;58:829–37.
[28] Partridge IK, Cartié DDR. Delamination resistant laminates by Z-fiber® pinning: part I manufacture and fracture performance. Compos Part A 2005;36(1):55–64.
[29] Mouritz AP, Leong KH, Herszberg I. A review of effect of stitching on the in-plane mechanical properties of fibre-reinforced polymer composites. Compos Part A 1999;28:979–91.
[30] Steeves CA, Fleck NA. In-plane properties of composite laminates with through-thickness pin reinforcement. Int J Solid Struct 2006;43:3197–212.
[31] Carlsson LA. Fracture of laminated composites with interleaves. In: Armanios E, editor. Fracture of composites key engineering materials, 120–121. Zurich: Trans Tech Publications; 1996. p. 489–520.
[32] Kim YA, Kamio L, Tajiri T, Hayashi T, Song SM, Endo M, et al. Enhanced thermal conductivity of carbon fiber/phenolic resin composites by the introduction of carbon nanotubes. Appl Phys Lett 2007;90:093125–7.
[33] Tong L, Tan P, Sun X. Effect of long multi-walled CNTs on delamination toughness of laminated composites. J Comp Mat 2008;42:5–23.